Journal of the Physical Society of Japan
Vol. 79, No. 3, March, 2010, 034710

Simultaneous Metal–Insulator and Spin-State Transition in $(Pr_{1-y}RE_y)_{1-x}Ca_xCoO_3$ (RE = Nd, Sm, Gd, and Y)

Tomoyuki NAITO*, Hiroko SASAKI, and Hiroyuki FUJISHIRO

Faculty of Engineering, Iwate University, 4-3-5 Ueda, Morioka 020-8551, Japan

(Received June 24, 2009; accepted December 18, 2009; published March 10, 2010)

We have studied a Pr-site substitution effect using various RE ions (RE = Nd, Sm, Gd, and Y) on a simultaneous metal–insulator (MI) and spin-state (SS) transition in $(Pr_{1-y}RE_y)_{1-x}Ca_xCoO_3$ using measurements of electrical resistivity, magnetization, and thermal dilatation. The MI–SS transition took place at the appropriate combination of x and y for samples of RE = Sm, Gd, and Y. The MI–SS transition temperatures $T_{MI\text{–}SS}$ can be scaled universally by the average ionic radius $\langle r_A \rangle$ of the A-site in the perovskite $ACoO_3$, which is independent of x, y, and the RE ion species. The atomic randomness of the A-site, which is defined as the mean square deviation σ^2, larger than the critical value σ_{cr}^2 is also necessary for the occurrence of the MI–SS transition and $T_{MI\text{–}SS}$ increases with increasing σ^2. In contrast, no MI–SS transition was observed in the RE = Nd samples ($x = 0.2-0.4$), which can be inferred from the small σ^2 value because of the small difference in ionic radius between Pr^{3+} and Nd^{3+}. The atomic randomness of the A-site might be an important parameter that dominates the MI–SS transition through the difference in electronic energy δE between the spin states of Co^{3+} ions.

KEYWORDS: Pr–Ca–Co–O system, metal–insulator transition, spin-state transition, tolerance factor, atomic randomness
DOI: 10.1143/JPSJ.79.034710

1. Introduction

In $RECoO_3$ (RE = rare-earth element), a spin-state (SS) transition of Co^{3+} ions from a low spin state (LS; $t_{2g}^6 e_g^0$, $S = 0$) to an intermediate spin state (IS; $t_{2g}^5 e_g^1$, $S = 1$) or a high spin state (HS; $t_{2g}^4 e_g^2$, $S = 2$) occurs with increasing temperature, which indicates a small difference in electronic energy δE between the LS and IS (or HS) states.[1–3] Among cobaltites, a first-order metal–insulator (MI) transition accompanying the SS transition was first reported in $Pr_{0.5}Ca_{0.5}CoO_3$ at ambient pressure.[4] Large volume contraction, mainly caused by the tilting of the CoO_6 octahedra below the transition temperature $T_{MI\text{–}SS}$, was also found.[4] The tilting of the CoO_6 octahedra decreases the bond angle of Co–O–Co, which weakens the covalency and thereby destabilizes the itinerant IS state. The ratio of Pr : Ca = 1 : 1 (Co^{3+} : Co^{4+} = 1 : 1) was thought to be apparently indispensable: a commensurate arrangement, such as a charge-ordering found in manganites,[5] plays a key role in the MI–SS transition. Later, however, the MI–SS transition was found in $Pr_{1-x}Ca_xCoO_3$ at $x \neq 0.5$ at a high pressure,[6] in which the charge-ordering was not confirmed through neutron diffraction studies.[6,7]

A similar transition was observed in $(Pr_{1-y}RE_y)_{1-x}Ca_xCoO_3$ with an appropriate combination of x and y at ambient pressure.[6,8] For $x = 0.5$, $T_{MI\text{–}SS}$ increased for samples with RE = Sm, Y, and Tb, but $T_{MI\text{–}SS}$ for the sample with a small amount of Nd substitution decreased concomitantly with increasing y. For $(Pr_{1-y}RE_y)_{0.7}Ca_{0.3}CoO_3$ (RE = Y, Tb), $T_{MI\text{–}SS}$ also increased concomitantly with increasing y. Both the large volume contraction of the unit cell and the decrease in Co–O–Co bond angle below $T_{MI\text{–}SS}$ indicated that the Co–Co transfer energy t was important for determining δE. However, the relationship between $T_{MI\text{–}SS}$ and the ionic radius of the substituting RE ion remains controversial. To clarify the substitution effect on the MI–SS transition in $(Pr_{1-y}RE_y)_{1-x}Ca_xCoO_3$, further systematic studies are necessary for various RE ions, x and y.

As described in this paper, we report the respective temperature dependences of the electrical resistivity and susceptibility of the polycrystalline $(Pr_{1-y}RE_y)_{1-x}Ca_xCoO_3$ samples (RE = Nd, Sm, Gd, and Y) for various x and y values, and discuss the relationship between the MI–SS transition and the distortion and atomic randomness in the crystal using various parameters, such as the tolerance factor Γ_t, the average ionic radius of the A-site $\langle r_A \rangle$, and the mean square deviation σ^2 of the A-site in $ACoO_3$ perovskite.

2. Experimental Procedure

Polycrystalline samples of $(Pr_{1-y}RE_y)_{1-x}Ca_xCoO_3$ (RE = Nd, Sm, Gd, and Y) were prepared using a solid-state reaction. Raw powders of Pr_6O_{11}, RE_2O_3, Co_3O_4, and $CaCO_3$ were weighted with appropriate molar ratios and ground using an agate mortar and pestle for 1 h. Mixed powders were calcined at 1000 °C for 24 h in air. They were pulverized and ground. Then, they were pressed into pellets of 20 mm diameter and 4 mm thickness. Pellets were sintered at 1200 °C for 24 h in 0.1 MPa flowing oxygen gas. The measured densities of each sample were greater than 90% of the ideal density. Powder X-ray diffraction patterns were taken for each sample using Cu Kα radiation; the samples were confirmed to have a single-phase orthorhombic (*Pbmn*) structure. Electrical resistivity was measured using a four-probe method with a parallelepiped sample cut from the pellet with a typical current density of 0.01 A/cm^2. Susceptibility was measured using a superconducting quantum interference device (SQUID) magnetometer (Quantum Design MPMS-XL). Thermal dilatation, $dL(T)/L(300\,K)$ [$= (L(T) - L(300\,K))/L(300\,K)$], based on the sample length at 300 K, was measured by a strain-gauge method.

*E-mail: tnaito@iwate-u.ac.jp

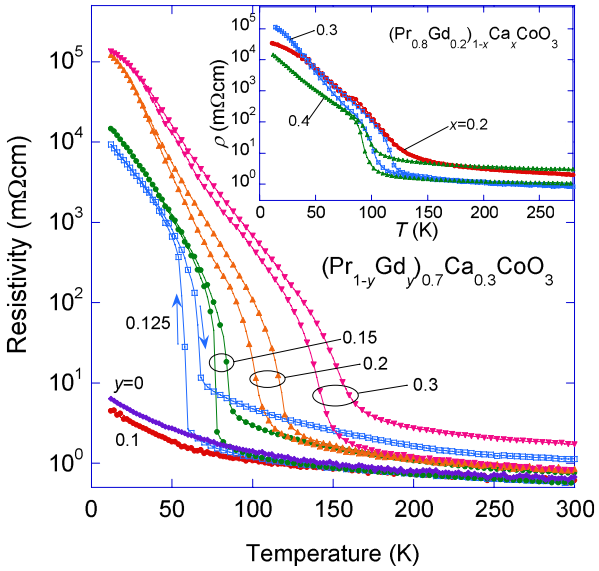

Fig. 1. (Color online) Temperature dependence of the resistivity $\rho(T)$ of the $(Pr_{1-y}Gd_y)_{0.7}Ca_{0.3}CoO_3$ samples for various y values. The inset shows the x dependence of $\rho(T)$ for the $(Pr_{0.8}Gd_{0.2})_{1-x}Ca_xCoO_3$ samples.

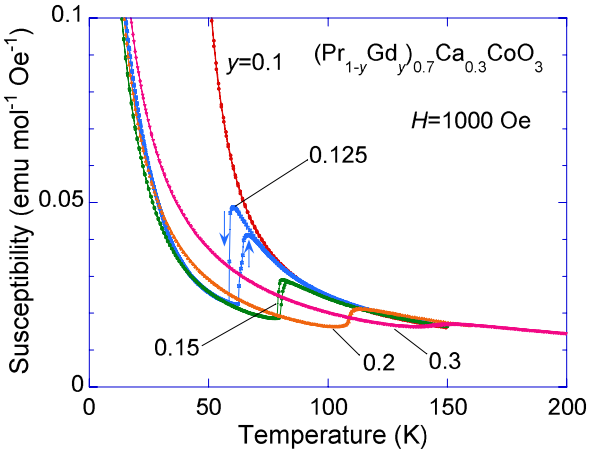

Fig. 2. (Color online) Temperature dependence of the susceptibility $\chi(T)$ under the field cooling and subsequent field warming of the $(Pr_{1-y}Gd_y)_{0.7}Ca_{0.3}CoO_3$ samples for various y values.

3. Results

Figure 1 shows the temperature dependence of the resistivity $\rho(T)$ of $(Pr_{1-y}Gd_y)_{0.7}Ca_{0.3}CoO_3$ for various y values. For $y = 0$ and 0.1, $\rho(T)$ increases moderately with decreasing temperature. We define $\rho(T)$ as a "metallic" behavior, as indicated in the previous report.[4] For $y = 0.125$, $\rho(T)$ shows a jump with two orders of magnitude at $T_{MI\text{–}SS} = 60$ K on the cooling run. In fact, $T_{MI\text{–}SS}$ was determined as the temperature at which the temperature derivative of the resistivity $d\rho/dT$ was maximum. On the heating run, $\rho(T)$ showed a sharp drop at $T_{MI\text{–}SS} = 70$ K. $T_{MI\text{–}SS}$ increases and the width of the transition broadens with increasing y. Consequently, the nature of the phase transition changes from first-order to second-order with decreasing ionic radius of the $(Pr_{1-y}Gd_y)$ site; the ionic radius of Gd^{3+} (0.1107 nm) is smaller than that of Pr^{3+} (0.1179 nm).[9] Such a difference in the ionic radius causes the local lattice distortion that results in the MI–SS transition through the energy balance between Hund coupling and crystal field splitting.[4,6] For $y = 0.125$, the absolute value of $\rho(T)$ on the heating run was larger than that on the cooling run above $T_{MI\text{–}SS}$. The irreversibility in the $\rho(T)$ values on the cooling and heating runs cannot be explained by the nature of the first-order phase transition. The discrepancy in ρ disappears for $y = 0.2$; however, it appears again for $y = 0.3$, which might come from the microcracks created by the large volume contraction and expansion passing through the transition temperature.[4] The microcracks might increase the $\rho(T)$ value on the heating run.

The inset of Fig. 1 shows the x dependence of $\rho(T)$ for $(Pr_{0.8}Gd_{0.2})_{1-x}Ca_xCoO_3$. The $\rho(T)$ curve of $x = 0.3$ is the same as that in the main panel in Fig. 1. For $x = 0.2$, the MI–SS transition is second-order-like. With increasing x, the absolute value of $\rho(T)$ decreases slightly, $T_{MI\text{–}SS}$ decreases, and the transition becomes sharper. In this manner, the $\rho(T)$ behavior depends not only on the ionic radius of the $(Pr_{1-y}Gd_y)$ site but also on the hole concentration x. The $T_{MI\text{–}SS}$ transition takes place at an appropriate combination of x and y values in $(Pr_{1-y}Gd_y)_{1-x}Ca_xCoO_3$.

Figure 2 shows the temperature dependence of the susceptibility $\chi(T)$ at $H = 1000$ Oe under field cooling, in addition to the subsequent field warming of the $(Pr_{1-y}Gd_y)_{0.7}Ca_{0.3}CoO_3$ samples presented in Fig. 1. For $y = 0.1$, $\chi(T)$ monotonically increases with decreasing temperature, depending on the Curie law. For $y = 0.125$, $\chi(T)$ shows a sharp drop on cooling and a sharp jump on warming at $T_{MI\text{–}SS}$, which are the same as those of the $\rho(T)$ shown in Fig. 1. The hysteretic $\chi(T)$ behavior shows the SS transition of Co^{3+} ions between the LS and IS (or HS) states at $T_{MI\text{–}SS}$. The hysteretic MI transition in $\rho(T)$ takes place simultaneously.[4,6] The anomalies in the $\chi(T)$ curve become small and broad with increasing y, which are similar to the y dependence of $\rho(T)$. In contrast to the $\rho(T)$ behavior, the $\chi(T)$ values above $T_{MI\text{–}SS}$ coincide exactly on cooling and heating runs. Although microcracks are created in the sample at the transition, $\chi(T)$ might not be affected because susceptibility has a microscopic origin. The result suggests that the discrepancy in $\rho(T)$ above $T_{MI\text{–}SS}$ arises from microcracks in the sample.

Figure 3 shows the temperature dependence of the thermal dilatation $dL(T)/L(300\,K)$ of the $(Pr_{1-y}Gd_y)_{0.7}Ca_{0.3}CoO_3$ samples. $dL(T)/L$ can detect the lattice anomalies. For $y = 0.1$, $dL(T)/L(300\,K)$ decreases monotonically with decreasing temperature and no anomaly appears down to 20 K. For $y = 0.125–0.3$, $dL(T)/L(300\,K)$ shows a large drop below $T_{MI\text{–}SS}$; for example, $dL(20\,K)/L(300\,K)$ for the $y = 0.15$ sample is -0.008, which is twice as large as that for the $y = 0.10$ sample. In general, a sharp drop in $dL(T)/L(300\,K)$ originates from the decrease in CoO_6 volume (V_o), Co–O–Co bond angle (α), or unit cell volume (V_u). In the previous studies,[4,6] abrupt decreases in V_u and α were observed below $T_{MI\text{–}SS}$. However, the V_o value increased slightly below $T_{MI\text{–}SS}$. In the present case, we consider that the sharp drop in $dL(T)/L(300\,K)$ comes from the decrease in α and/or the decrease in V_u. The abrupt dilatation broadens with increasing y similarly to the transition in $\rho(T)$ and $\chi(T)$. A large dilatation is the origin of the irreversibility in $\rho(T)$ above $T_{MI\text{–}SS}$ shown in Fig. 1.

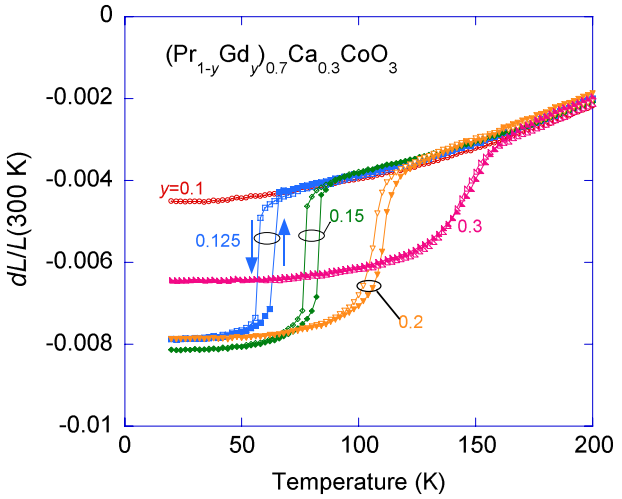

Fig. 3. (Color online) Temperature dependence of the thermal dilatation $dL(T)/L(300\,\mathrm{K})$ of the $(Pr_{1-y}Gd_y)_{0.7}Ca_{0.3}CoO_3$ samples for various y values.

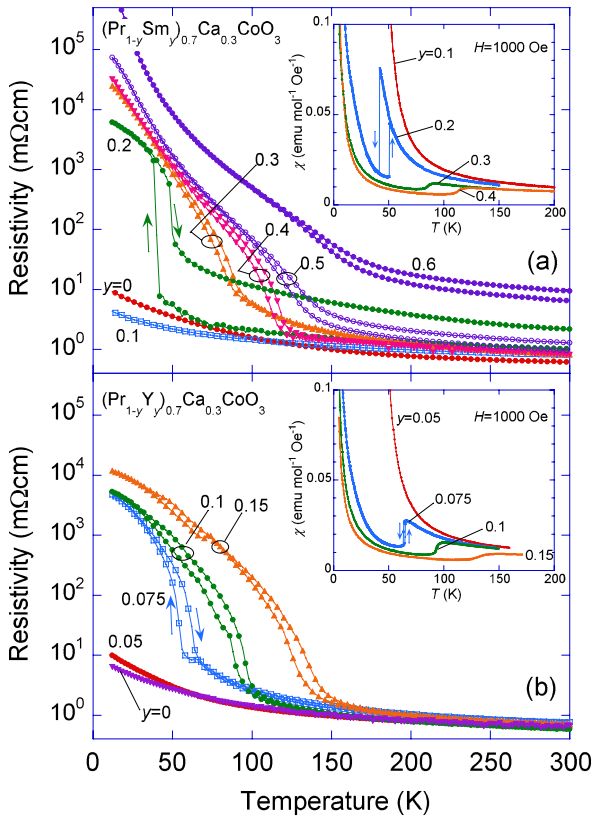

Fig. 4. (Color online) Temperature dependence of the resistivity (main panel) $\rho(T)$ and susceptibility (inset) $\chi(T)$ of the (a) $(Pr_{1-y}Sm_y)_{0.7}Ca_{0.3}CoO_3$ and (b) $(Pr_{1-y}Y_y)_{0.7}Ca_{0.3}CoO_3$ samples for various y values.

We measured the $\rho(T)$ and $\chi(T)$ of both $(Pr_{1-y}Sm_y)_{0.7}Ca_{0.3}CoO_3$ and $(Pr_{1-y}Y_y)_{0.7}Ca_{0.3}CoO_3$ series for various y values, as presented in Figs. 4(a) and 4(b). The insets show $\chi(T)$. The ionic radii of Sm^{3+} (0.1132 nm) and Y^{3+} (0.1075 nm) are smaller than that of Pr^{3+} (0.1179 nm).[9] Actually, $\rho(T)$ and $\chi(T)$ in both series are similar to those in $(Pr_{1-y}Gd_y)_{0.7}Ca_{0.3}CoO_3$; the MI–SS transition is observed in $y = 0.2$–0.6 for $(Pr_{1-y}Sm_y)_{0.7}Ca_{0.3}CoO_3$ and in $y = 0.075$–0.15 for $(Pr_{1-y}Y_y)_{0.7}Ca_{0.3}CoO_3$. Furthermore, $T_{MI\text{–}SS}$ increases, and the width of the transition broadens with increasing y. The critical substitution concentration y_{cr}, at which the MI–SS transition emerges, decreases concomitantly with decreasing ionic radius of the substituting RE ion.

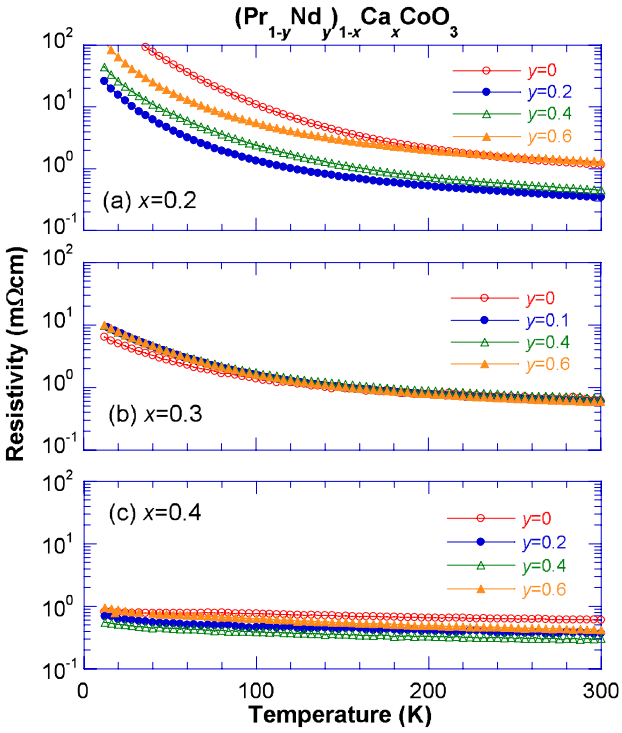

Fig. 5. (Color online) Temperature dependence of the resistivity $\rho(T)$ of the $(Pr_{1-y}Nd_y)_{1-x}Ca_xCoO_3$ samples ($x = 0.2$, 0.3, and 0.4) for various y values.

Figure 5 shows the temperature dependence of the $\rho(T)$ of $(Pr_{1-y}Nd_y)_{1-x}Ca_xCoO_3$ samples ($x = 0.2$, 0.3, and 0.4) for various y values. In fact, the absolute value of $\rho(T)$ decreased with increasing x. The $\rho(T)$ for $x = 0.3$ and 0.4 was independent of temperature or increased slightly with decreasing temperature, similarly to a metallic behavior. No discontinuous transition was observed in all the Nd-substituted samples studied. The absolute value of $\rho(T)$ seems to be independent of the y value up to $y = 0.6$. The absence of the MI–SS transition arises from the small difference in ionic radius between Nd^{3+} (0.1163 nm) and Pr^{3+} (0.1179 nm);[9] the physical properties of $(Pr_{1-y}Nd_y)_{1-x}Ca_xCoO_3$ are similar to those of $Pr_{1-x}Ca_xCoO_3$ and $Nd_{1-x}Ca_xCoO_3$, neither of which shows the MI–SS transition, even at high pressures of up to 10 GPa.[8,10] Fujita *et al.* reported that the MI–SS transition occurred in $(Pr_{1-y}Nd_y)_{0.5}Ca_{0.5}CoO_3$ for $0 \le y \le 0.1$ at ambient pressure and $T_{MI\text{–}SS}$ decreased concomitantly with increasing y.[6] In the next section, we discuss the relationship between the MI–SS transition and various parameters, such as the species of the substituting RE ion, the concentration of the substituted RE ion y, and the Ca concentration x in the $(Pr_{1-y}RE_y)_{1-x}Ca_xCoO_3$ system.

4. Discussion

As described in the preceding section, the MI–SS transition was not observed in $(Pr_{1-y}Nd_y)_{1-x}Ca_xCoO_3$ for $0 \le y \le 0.6$ and $0.2 \le x \le 0.4$; however, it was observed in $(Pr_{1-y}Sm_y)_{0.7}Ca_{0.3}CoO_3$ for $0.2 \le y \le 0.6$, although

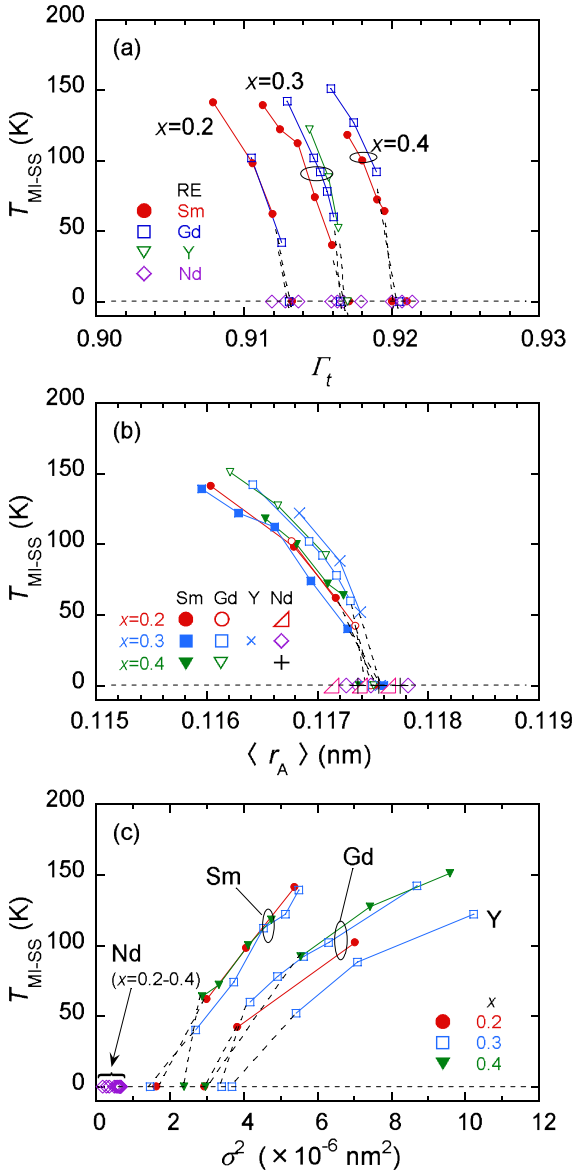

Fig. 6. (Color online) MI–SS transition temperature T_{MI-SS} as a function of (a) the tolerance factor Γ_t, (b) the average ionic radius of A-site $\langle r_A \rangle$, and (c) the mean square deviation σ^2.

the difference in ionic radius between Sm^{3+} (0.1132 nm) and Nd^{3+} (0.1163 nm) is only about 3%. Furthermore, the $(Pr_{1-y}RE_y)_{0.7}Ca_{0.3}CoO_3$ samples (RE = Sm, Gd, and Y) showed no MI–SS transition for $y < y_{cr}$. We discuss why the MI–SS transition does not occur in these cases. First, we consider the relationship between the MI–SS transition and the tolerance factor Γ_t, which defines the lattice distortion as follows:

$$\Gamma_t = \frac{\langle r_A \rangle + r_O}{\sqrt{2}(\langle r_B \rangle + r_O)}, \quad (1)$$

where $\langle r_A \rangle$, $\langle r_B \rangle$, and r_O respectively denote the average ionic radii of the A-site $[(Pr_{1-y}RE_y)_{1-x}Ca_x]$, B-site (Co), and O in the ABO_3 perovskite oxide.

Figure 6(a) shows the relationship between T_{MI-SS} determined in the cooling run and Γ_t for all samples measured in this study. $\langle r_A \rangle$ in eq. (1) was calculated using the relation

$$\langle r_A \rangle = [(1-x)(1-y)] \times r_{Pr} + [(1-x)y] \times r_{RE} + x \times r_{Ca}.$$

$\langle r_B \rangle = r_{Co}$ was estimated as $\langle r_B \rangle = x \times r_{Co^{4+}} + (1-x) r_{Co^{3+}}$ using $r_{Co^{3+}}$ (0.061 nm) and $r_{Co^{4+}}$ (0.053 nm).[9] For the sample showing no transition, T_{MI-SS} is defined as zero. In Fig. 6(a), for each x, T_{MI-SS} decreases monotonically with increasing Γ_t, i.e., with increasing relaxation of the local lattice distortion. The T_{MI-SS} vs Γ_t plot is independent of both the y value and the species of substituting RE ions (RE = Sm, Gd, and Y), and shifts to the right with increasing x. This result mainly arises from the large difference in ionic radius between Co^{3+} and Co^{4+}; the Γ_t value increases concomitantly with decreasing x because of $r_{Co^{4+}} < r_{Co^{3+}}$.

Figure 6(b) shows the relationship between T_{MI-SS} and $\langle r_A \rangle$ for the same samples presented in Fig. 6(a). All plots except for RE = Nd can be represented roughly on a universal line that is independent of x and y values, and the RE ion species. These results indicate that T_{MI-SS} depends strongly on the $\langle r_A \rangle$ value. For example, for $(Pr_{1-y}Nd_y)_{0.7}Ca_{0.3}CoO_3$ ($y = 0.4$) without MI–SS transition, the Γ_t value of 0.916 is the same as that of $(Pr_{1-y}Sm_y)_{0.7}Ca_{0.3}CoO_3$ ($y = 0.2$), which shows the MI–SS transition at 42 K. From the viewpoint of the Γ_t value, $(Pr_{0.6}Nd_{0.4})_{0.7}Ca_{0.3}CoO_3$ should show the MI–SS transition. Even if T_{MI-SS} is universally scaled as a function of $\langle r_A \rangle$ for the RE-substituted system (RE = Sm, Gd, and Y), the absence of the MI–SS transition in the Nd-substituted system cannot be explained. To clarify the absence of the transition in Nd-substituted samples, we must introduce another parameter.

The substitution of the RE and/or Ca ions for the Pr ions would introduce atomic randomness in the A-site in addition to the local distortion in the lattice. The atomic randomness of the A-site is defined as the mean square deviation

$$\sigma^2 = \sum y_i r_i^2 - \langle r_A \rangle^2,$$

where y_i and r_i respectively stand for the concentration and ionic radius of each element in the A-site. Figure 6(c) shows plots of T_{MI-SS} vs σ^2 for all samples in this study. For each x and each substituted RE ion (RE = Sm, Gd, and Y), T_{MI-SS} monotonically decreases concomitantly with decreasing σ^2 and reaches zero for σ^2 lower than the critical value σ^2_{cr}. It is noteworthy that the T_{MI-SS} vs σ^2 plots are scaled for each substituted RE ion and are independent of x and y. The σ^2 values of the $(Pr_{1-y}Nd_y)_{1-x}Ca_xCoO_3$ samples ($0.2 \le x \le 0.4$ and $0 \le y \le 0.6$) are estimated to be $(0.5-0.7) \times 10^{-6}$ nm^2, which are smaller than the critical σ^2_{cr} value. An atomic randomness in the A-site larger than σ^2_{cr} is necessary for the occurrence of the MI–SS transition, although the lattice distortion defined by the tolerance factor Γ_t is satisfied. A possible origin of the MI–SS transition related to σ^2 is the structural inhomogeneity due to the local atomic randomness that introduces the fluctuation in energy balance between Hund coupling and crystal field splitting.

Recently, Tong *et al.*[7] have suggested the importance of distortion in the CoO_6 octahedra in causing the MI–SS transition by comparing $Pr_{0.5}Ca_{0.5}CoO_3$ and $Pr_{0.5}Ca_{0.5}CoO_{3-\delta}$ ($\delta \sim 0.045$); the oxygen deficiency relaxed the distortion in the CoO_6 octahedra, and then, the transition vanished. The local distortion in the CoO_6 octahedra enhances electron–phonon coupling, which suppresses the itinerant nature of the e_g electrons. Wang *et al.*[11] reported the oxygen isotope effect on the MI–SS transition in $(Pr_{0.7}Sm_{0.3})_{0.7}Ca_{0.3}CoO_3$. Actually, the T_{MI-SS} of the sample

with ^{18}O was higher than that of the sample with ^{16}O. This result is explained by the increase in the electron mass m^* of the sample with ^{18}O because of the enhanced electron–phonon coupling, which increased δE and decreased the Co–Co transfer energy t. Fujita *et al.* studied the MI–SS transition of the $(Pr_{1-y}RE_y)_{0.5}Ca_{0.5}CoO_3$ samples at ambient pressure.[6] Actually, the T_{MI-SS} of the sample with RE = Sm, Y, and Tb was higher, but that of the sample with RE = Nd was lower than that of $Pr_{0.5}Ca_{0.5}CoO_3$. Because all the ionic radii of the above-described RE ions are smaller than that of Pr^{3+}, the substitution effect on the shift in T_{MI-SS} should be apparently similar. However, the results obtained in this study contradicted those obtained by Fujita *et al.* for the Nd-substituted samples. From the results of this study, we infer that the ionic radius of Nd^{3+} ions is similar to that of Pr^{3+} ions and that the atomic randomness in the A-site is necessary for the occurrence of the MI–SS transition. The samples used in this study were fabricated at ambient pressure in the flowing gas. Our samples were different from the samples prepared by Fujita *et al.*, which were annealed in high-pressure oxygen atmosphere. The difference in oxygen content between the samples is one of the reasons for the different results of the Nd-substituted samples. The reason why both the Pr and Ca ions are necessary for the occurrence of the MI–SS transition has not yet been understood in the Pr–Ca–Co–O system.

5. Conclusions

To study the origin of the simultaneous metal–insulator (MI) and spin-state (SS) transition in a Pr–Ca–Co–O system, we measured the temperature dependences of the electrical resistivity and susceptibility of polycrystalline $(Pr_{1-y}RE_y)_{1-x}Ca_xCoO_3$ samples (RE = Nd, Sm, Gd, and Y) for $x = 0.2$, 0.3, and 0.4. Important experimental results and conclusions are summarized as follows.

(1) The MI–SS transition was observed in samples with RE = Sm, Gd, and Y at an appropriate combination of x and y. The MI–SS transition temperature T_{MI-SS} increases concomitantly with increasing y for each x. However, the MI–SS transition was not realized for $(Pr_{1-y}Nd_y)_{1-x}Ca_xCoO_3$ $(0.2 \leq x \leq 0.4, 0 \leq y \leq 0.6)$.

(2) Actually, T_{MI-SS} can be scaled by the tolerance factor Γ_t for each x, which is independent of the species of RE ions (RE = Sm, Gd, and Y). The relationship between T_{MI-SS} and the average ionic radius $\langle r_A \rangle$ of the $[(Pr_{1-y}RE_y)_{1-x}Ca_x]$ site can be scaled universally, which is independent of the species of RE ions and the concentrations of x and y. These results suggest that T_{MI-SS} strongly depends on the local distortion in the lattice. However, the absence of the MI–SS transition in the Nd-substituted sample cannot be explained from the viewpoints of Γ_t and $\langle r_A \rangle$.

(3) In fact, T_{MI-SS} can be scaled by the atomic randomness of the A-site, which is defined as the mean square deviation σ^2 for each RE ion (RE = Sm, Gd, and Y), which is independent of x and y. An atomic randomness larger than the critical value of σ^2_{cr} is expected to be necessary in the A-site for the occurrence of the MI–SS transition by the introduction of the fluctuation in energy balance. Because the ionic radius of Pr^{3+} is similar to that of Nd^{3+}, the σ^2 value of $(Pr_{1-y}Nd_y)_{1-x}Ca_xCoO_3$ is smaller than those of other RE-substituted samples. A σ^2 smaller than σ^2_{cr} is a possible explanation for the absence of the MI–SS transition in the Nd-substituted sample.

Acknowledgments

The authors acknowledge Dr. J. Hejtmanek of Czech Republic for valuable discussions and Ms. M. Ishida of Iwate University for performing part of the experiments. We are grateful to Dr. S. Kobayashi for his cooperation in magnetization measurements, which were performed at the Non-Destructive Evaluation and Science Research Center, Faculty of Engineering, Iwate University.

1) P. M. Raccah and J. B. Goodenough: Phys. Rev. **155** (1967) 932.
2) M. A. Korotin, S. Yu. Ezhov, I. V. Solovyev, V. I. Anisimov, D. I. Khomskii, and G. A. Sawatzky: Phys. Rev. B **54** (1996) 5309.
3) J.-Q. Yan, J.-S. Zhou, and J. B. Goodenough: Phys. Rev. B **69** (2004) 134409.
4) S. Tsubouchi, T. Kyomen, M. Itoh, P. Ganguly, M. Oguni, Y. Shimojo, Y. Morii, and Y. Ishii: Phys. Rev. B **66** (2002) 052418.
5) Y. Tomioka, A. Asamitsu, Y. Moritomo, H. Kuwahara, and Y. Tokura: Phys. Rev. Lett. **74** (1995) 5108.
6) T. Fujita, T. Miyashita, Y. Yasui, Y. Kobayashi, M. Sato, E. Nishibori, M. Sakata, Y. Shimojo, N. Igawa, Y. Ishii, K. Kakurai, T. Adachi, Y. Ohishi, and M. Takata: J. Phys. Soc. Jpn. **73** (2004) 1987.
7) P. Tong, Y. Wu, B. Kim, D. Kwon, J. M. S. Park, and B. G. Kim: J. Phys. Soc. Jpn. **78** (2009) 034702.
8) T. Fujita, S. Kawabata, M. Sato, N. Kurita, M. Hedo, and Y. Uwatoko: J. Phys. Soc. Jpn. **74** (2005) 2294.
9) R. D. Shanon: Acta Crystallogr., Sect. A **32** (1976) 751.
10) S. Tsubouchi, T. Kyomen, M. Itoh, and M. Oguni: Phys. Rev. B **69** (2004) 144406.
11) G. Y. Wang, T. Wu, X. G. Luo, W. Wang, and X. H. Chen: Phys. Rev. B **73** (2006) 052404.